Quasi-hydrostatic x-ray powder diffraction study of the low- and high-pressure phases of $CaWO_4$ up to 28 GPa

R. Vilaplana[1], R. Lacomba-Perales[2], O. Gomis[1], D. Errandonea[2], Y. Meng[3]

[1]Centro de Tecnologías Físicas, MALTA Consolider Team, Universitat Politècnica de València, 46022 València, Spain. **E-mail: rovilap@fis.upv.es**

[2]Departamento de Física Aplicada-ICMUV, Universidad de Valencia, MALTA Consolider Team, Edificio de Investigación, C/Dr. Moliner 50, 46100 Burjassot, Spain

[3]HPCAT, Carnegie Institution of Washington, Bldg. 434E, 9700 S. Cass Avenue, Argonne, IL 60439, USA

Abstract: We have studied $CaWO_4$ under compression using Ne as pressure-transmitting medium at room temperature by means of synchrotron x-ray powder diffraction. We have found that $CaWO_4$ beyond 8.8 GPa transforms from its low-pressure tetragonal structure (scheelite) into a monoclinic structure (fergusonite). The high-pressure phase remains stable up to 28 GPa and the low-pressure phase is totally recovered after full decompression. The pressure dependence of the unit-cell parameters, as well as the pressure-volume equation of state, has been determined for both phases. Compared with previous studies, we found in our quasi-hydrostatic experiments a different behavior for the unit-cell parameters of the fergusonite phase and a different transition pressure. These facts suggest that deviatoric stresses influence on the high-pressure structural behavior of $CaWO_4$ as previously found in related compounds. The reported experiments also provide information on the pressure dependence of interatomic bond distances, shedding light on the transition mechanisms.

Keywords: high pressure, calcium tungstate, scheelite, x-ray diffraction, phase transition.

PACS number(s): 62.50.-p, 61.50.Ks, 61.05.cp, 63.20.dd

Introduction

Scheelite is a calcium tungstate mineral with chemical formula $CaWO_4$. At ambient pressure (10^{-4} GPa) and room temperature (RT), it crystallizes in a tetragonal structure with space group (SG) $I4_1/a$, Z = 4. Many orthotungstates, orthomolybdates **[1]**, and other compounds are crystallographically isostructural to scheelite. They are technologically important materials and have a long history of practical application. Among various applications, orthotungstates are used as solid-state scintillators **[2,3]**, laser-host materials **[4]**, and in optoelectronic devices **[5–7]**. In particular, due to their large x-ray absorption coefficient and scintillation output, orthotungstates are very popular for detecting x-rays and γ-rays in medical applications.

The scheelite structure can be described as a highly ionic crystal with Ca^{+2} cations and tetrahedral WO_4^{-2} anions forming a cubic close-packed array **[1]**. It can be visualized as an assembly of isolated WO_4 tetrahedra that are corner connected by CaO_8 dodecahedra **[8]**. **Fig. 1** illustrates the scheelite structure, which can be also seen as two intercalated diamond lattices, one for Ca atoms and other for W atoms. This results in a layered stacking in which the O atoms are connected with two Ca and one W.

After the pioneer work of Nicol and Durana **[9]**, several high-pressure (HP) studies have been performed in scheelite-type tungstates **[10-22]**. They showed that compression is an efficient tool to improve the understanding of their physical properties **[23]**. Based upon Raman measurements, Nicol and Durana **[9]** discovered a pressure-induced transition at 1.5 GPa in $CaWO_4$. This study was carried out using NaCl as pressure-transmitting medium (PTM). The authors proposed a monoclinic wolframite structure (SG: $P2/c$, Z = 2) for the HP phase. Later Raman experiments, using a 4:1 methanol-ethanol mixture as PTM, located the transition at 10 GPa **[10,11]**. Energy-dispersive x-ray powder diffraction (EDXRD) experiments in $CaWO_4$ were performed at the beginning of the present century **[12].** They

were carried out without PTM and the wolframite structure was assigned as the HP phase of $CaWO_4$. However, posterior angle-dispersive x-ray powder diffraction (ADXRD) measurements found the HP structure of $CaWO_4$ to be fergusonite (SG: *I2/a*, Z = 4) **[13]**. Helium (He) or a 4:1 methanol-ethanol mixture was used as PTM in these experiments. This conclusion was confirmed by subsequent ADXRD experiments done using silicone oil as PTM **[14]**. It was also supported by *ab initio* total-energy calculations and x-ray absorption near-edge structure measurements **[14,16]**. However, a more recent EDXRD study, performed using 16:3:1 methanol-ethanol-water as PTM **[19]**, concluded that scheelite $CaWO_4$ transforms to the wolframite structure. The above described results evidence that more efforts are needed to accurately determine the HP structural behavior of $CaWO_4$.

It is well known that the use of different PTM generates, in a diamond-anvil cell (DAC) and other HP devices, not only hydrostatic pressure but also deviatoric stress components **[24,25]**. Deviatoric stresses usually influence the HP structural behavior of materials **[26]**. In the particular case of scheelite-type oxides, the different deviatoric stresses caused by the use of different PTM leaded to discrepancies in the determination of the crystal structure of the HP phases **[22,27]**. This could be probably the cause of the finding of either the fergusonite or wolframite structure in $CaWO_4$ in different HP experiments. To clarify this issue, we performed an ADXRD study on $CaWO_4$ up to 28 GPa under quasi-hydrostatic conditions using neon (Ne) as PTM. The reported results will be compared with previous measurements carried out under several pressure environments. In particular, we will provide convincing evidence that beyond 8.8 GPa the scheelite structure transforms to fergusonite. The axial and bond compressibilities and the pressure-volume (P-V) equation of state (EOS) of $CaWO_4$ will also be presented. Our results are relevant for the understanding of the HP behavior of materials isomorphic to scheelite.

Experimental Details

Powder $CaWO_4$ samples used in the present experiments were obtained from a high-purity $CaWO_4$ single crystal, which was grown by Czochralski method **[5]**. The HP experiments were performed using a symmetric DAC. The culet size of diamond anvils was 400 μm and T301 stainless steel served as gasket material. The gasket was preindented to a thickness of 40 μm and a hole with a diameter of 100 μm was drilled in its center to act as pressure chamber. The sample together with a ruby ball was loaded into this chamber. Ne was used as PTM and pressure was determined from ruby fluorescence **[28]**.

HP ADXRD measurements were carried out at the 16-IDB station of HPCAT at the Advanced Photon Source (APS). Monochromatic synchrotron radiation with a wavelength of 0.40695 Å was employed. X-ray powder diffraction (XRD) was collected using a MAR345 image-plate detector located at 349.9 mm from the sample. The x-ray beam was focused down to 5 x 5 μm^2 using Kirkpatrick-Baez mirrors. The acquisition time was 20 seconds for each pressure. FIT2D was used to convert the collected two-dimensional XRD images into one-dimensional intensity versus 2θ diffraction patterns **[29]**. Indexing, structure solution, and refinements were performed using UNITCELL **[30]**, POWDERCELL **[31]**, and GSAS **[32]**.

Results and Discussion

Fig. 2 shows a selection of diffraction patterns of $CaWO_4$. These patterns can be assigned to the scheelite structure up to 8.8 GPa which is illustrated in the figure by the patterns measured at 0.3 and 7 GPa. Upon further compression the XRD patterns change indicating the occurrence of a structural phase transition. This can be seen in **Fig. 2** by comparing the patterns measured at 7 and 10.4 GPa. As we will show below, the XRD patterns measured from 10.4 to 28 GPa can be assigned to the fergusonite structure. Upon decompression to ambient pressure, the scheelite structure is fully recovered (see **Fig. 2**).

The transition pressure is more than 1 GPa smaller than the transition pressure reported in less hydrostatic experiments **[13,14]**. Rietveld refinements obtained for the low- and high-pressure phases at pressures of 0.3 and 24.6 GPa, respectively, are shown in **Fig. 2** together with the measured patterns. The small R-factors and residuals (see **Table I** and **Fig. 2**) support the assignation of the scheelite structure for the low-pressure phase up to 8.8 GPa and of the fergusonite structure to the HP phase. Note that in the XRD patterns, in addition to the Bragg reflections of the sample there are peaks assigned to Ne. One of them is marked with arrows in **Fig. 2** and can be easily identified. Another fact to remark is that no evidence of a second transition is found in our experiments up to 28 GPa. This is consistent with theoretical calculations **[14]** which predict a transition from fergusonite to an orthorhombic structure at 29 GPa.

Since the occupancy and the atomic displacement factors are correlated and sensitive to background subtraction **[33],** in order to reduce the number of free parameters in the refinement, the occupancies of all atoms were constrained to 1 as established by stoichiometry. The isotropic displacement parameters were fixed as 0.5 $Å^2$ **[33]**. In addition to the unit-cell parameters, for scheelite we also refined the oxygen atom positions (Ca and W positions are fixed by the structure symmetry). The oxygen atom positions were determined at the lowest pressure (0.3 GPa) without imposing any restraint. At higher pressure we used the oxygen atom positions obtained at 0.3 GPa as initial values for the refinements. We found that, within the pressure range of stability of the scheelite structure, the pressure changes in the oxygen atom internal parameters were comparable with experimental uncertainties. In the case of fergusonite, the positions of Ca, W, and O were refined **[14]**. **Table I** provides the structural parameters obtained from the Rietveld refinements at 0.3 and 24.6 GPa and the ambient pressure structural parameters obtained from literature **[34]**. The atomic positions obtained from the refinement at 0.3 GPa are

similar to the ambient pressure parameters **[34]**. Those refined for the fergusonite structure are similar to the atomic positions given in **Ref. [14]**.

In order to clearly show the qualitative differences between the XRD patterns of scheelite and fergusonite and to demonstrate that our HP phase cannot be explained by a wolframite structure, in **Fig. 3** we show two sequences of XRD patterns. The inset shows a series of XRD patterns measured in the scheelite phase plus one at 10.4 GPa corresponding to our first measurement of the HP phase. The angular region was chosen to highlight two typical features of the scheelite to fergusonite transition: The splitting of the (101) Bragg peak of scheelite into two peaks and the separation of (112) and (103) reflections of scheelite **[13]**. The other sequence showed in **Fig 3** is a selection of XRD patterns of the HP phase in the range 2θ = 3º-12º. There, it can be seen another distinctive feature of the fergusonite phase: the appearance at low-angles of a weak peak assigned to the (020) reflection of fergusonite. Over the XRD pattern measured at 24.6 GPa, the calculated position for Bragg reflections assuming the fergusonite structure are shown. At $2\theta < 10^{o}$ their Miller indices are indicated. At $2\theta > 10^{o}$ they are omitted to avoid overcrowding of the figure. Below the ticks corresponding to the peaks of fergusonite, we also give those calculated assuming the wolframite structure reported for $CaWO_4$ in the literature **[12]**. Clearly, there are several Bragg peaks of the HP phase that cannot be explained by the wolframite structure. Additionally, this structure implies the existence of two Bragg peaks near 6.5º which are not observed in our experiments.

We will discuss now the behaviour of scheelite in its stability range. From the measured patterns, we obtained the pressure dependence of the unit-cell parameters. In **Fig. 4** we show these results, and the pressure dependence of unit cell volume and axial ratio *c/a* obtained for the scheelite phase compared with previous results. It can be observed that our results (circles) follow a slightly different behavior from those previously reported **[8,13,14]**

in the experiments where the scheelite-fergusonite transition was found. It is worthy to note here that the two experiments **[12,19]** in which the behavior in *a* parameter versus pressure most differs from the tendencies showed in the rest of experiments, evolves at HP towards the wolframite phase. The behavior of the *c*-axis in the experiment of **Ref. 19** is also quite different from the other experiments. This anomalous pressure evolution of lattice parameters can be caused by experimental drawbacks like the sample bridging the anvils which will induce an increase a non-hydrostatic stresses **[35-37]**.

From our pressure-volume curve, we obtained the EOS for the scheelite phase using a second-order Birch-Murnaghan (BM) EOS **[38].** In **Table II**, the bulk modulus (B_0), its pressure derivative (B_0'), and the unit-cell volume at zero pressure (V_0) are summarized and compared with previous studies. In order to better compare our experiment with previous studies, we have refitted part of the earlier P-V data using a second-order BM EOS. The results are given in **Table II**. There, it can be seen that the present bulk modulus is 10% smaller than that obtained without PTM. On the other hand, our bulk modulus is 10% larger than the value determined using He as PTM **[13]** and from single-crystal experiments done under methanol-ethanol-water in a pressure range where this PTM behaves quasi-hydrostaticaly **[8]**. These two values are those that better agree with *ab initio* calculations **[14]**. On the other hand, our bulk modulus agrees within error bars with the values determined from powder samples in the experiments where organic compounds were used as PTM. This fact confirms that the compressibility of scheelite-type oxides is influenced by non-hydrostaticity as found in $BaWO_4$ **[22]**. From the results summarized in **Fig. 4**, we also obtained the axial compressibilities ($\kappa_x = \frac{-1}{x}\frac{\partial x}{\partial P}$) κ_a and κ_c. The values obtained by fitting the pressure evolution of *c* and *a* with a Murnaghan EOS **[39]** are κ_a = 2.3(1)·10^{-3} GPa^{-1} and κ_c = 3.6(1)·10^{-3} GPa^{-1}; thus κ_c/κ_a = 1.6(1). This fact implies that the anisotropy of

the scheelite structure decreases under compression. In our case *c*/*a* changes from 2.168(5) at 0.3 GPa to 2.140(5) at 8.8 GPa. As can be seen in **Fig. 4**, some of previous experiments give a similar pressure evolution for the axial ratio than the present experiment. However; we found that two experiments are noticeably different. The first one is the experiment done without PTM **[12]** in which the change of *c/a* almost doubles the value obtained in the rest of the experiments. The second one is the experiment of **Ref. 19** in which a very unusual pressure behavior is reported for *c/a*. In this experiment, deviatoric stresses were large (as commented above) and obviously in the experiment carried out without PTM too. Thus, deviatoric stresses not only influence the bulk compressibility but also the anisotropic behavior of $CaWO_4$. Notice that also both experiments are the only exception where $CaWO_4$ evolves at HP towards wolframite.

We will discuss now the bond compressibility in the scheelite structure. Theoretical calculations **[14]** and a high-temperature study **[40]** have established that the WO_4 tetrahedron behaves as a rigid unit, and the expansion/contraction of the scheelite is dominated by the change of Ca-O bonds. From our experiments we have calculated the evolution of W-O and Ca-O distances up to 8.8 GPa. In the **Fig. 5** we show a comparison of our results with those extracted from previous experiments. From our results we have calculated the bond compressibilities of the W-O and Ca-O bonds corresponding to the WO_4 tetrahedron and the CaO_8 dodecahedron. These compressibilities ($k_d = -\frac{1}{d}\frac{\partial d}{\partial P}$, where d is the bond distance) have been calculated assuming a linear evolution for the bond lengths. We obtained for the W-O bond length a compressibility of 2.8(1) 10^{-3} GPa^{-1}, for the short Ca-O bond length a value of 3.0(2) 10^{-3} GPa^{-1}, and for the long Ca-O bond length a value of 3.5(3) 10^{-3} GPa^{-1}. From these values and **Fig. 5** some conclusions can be extracted. First, only the early single-crystal experiment **[8]** and the non-hydrostatic experiment **[12]** found that W-O distances are highly incompressible. In contrast, according to the present and

previous ADXRD experiments **[13,14]** the difference between Ca-O and W-O bond compressibilities is only 12%. Second, since Ca-O bonds are 50% larger than W-O bonds, the change induced by pressure in the Ca-O bonds causes larger changes in the crystal structure. As a consequence of it and also due to the way the CaO_8 dodecahedra are linked (see **Fig. 1**) the compression of the *c*-axis is larger than that of the *a*-axis. Third, within the accuracy of the experiments, it cannot be definitively determined whether the CaO_8 dodecahedron becomes more regular under compression or not.

We will discuss now the changes induced by pressure in the crystal structure of the HP phase of $CaWO_4$. In **Fig. 6** the pressure evolution of the unit-cell parameters, the unit-cell volume, and the axial ratio are compared with previous experiments and with the low-pressure phase **[8, 12-14, 19]**. At the phase transition, we found that the *a* and *c* lattice parameters of fergusonite diverge more rapidly from the *a* lattice parameter of scheelite than in the experiment carried our using silicone oil as PTM. We consequently detect a discontinuity in the volume that was not previously observed in other experiments where the scheeelite-to-fergusonite phase transition occurs. The contraction of the volume at the transition is ~1%. In addition, **Fig. 6** shows that the HP phase is less compressible than the scheelite phase. Another fact to remark is that we found a non-linear behavior of the unit-cell parameters. In particular, beyond 12 GPa the *a*-axis of fergusonite, which in the first compression steps increases upon compression, bends towards the pressure axis. The change on the behavior of the *a*-axis implies a reduction of the spontaneous strain induced in the monoclinic structure beyond 15 GPa [17]. It is noticeably that a similar non-linear behavior of Raman phonons has been observed in fergusonite $CaWO_4$ [11], changing the evolution of Raman modes at the same pressure where we observed the change of the pressure dependence of the unit-cell parameter *a*. For the fergusonite phase we have also determined an EOS, with the parameters V_0 = 308(2) $Å^3$, B_0 = 93(4) GPa, and B_0' = 4 (fixed). Another

fact that can be seen in **Fig. 6** is that the β angle of fergsuonite gradually increases upon compression and that the axial ratios *b/a* and *b/c* follow a nonlinear evolution. Both facts lead to an enhancement of the monoclinic distortion of fergusonite.

Under compression $CaWO_4$ has been identified in three different polymorphs: scheelite, fergusonite, and wolframite. Wolframite has been only observed in experiments done under highly non-hydrostatic conditions **[12, 19]**. In Ref **[13]** it was stated that wolframite could have been misidentified in previous works. Consequently we have considered that possibility. We found that XRD patterns assigned to wolframite in Refs. **[12]** and **[19]** cannot be indexed with the fergusonite structure because it fails to explain many of the observed Bragg peaks. In contrast, the XRD patterns can be fit with the wolframite structure. Thus, we will consider for the next discussion that wolframite $CaWO_4$ can be obtained under non-hydrostatic pressure. In spite of that, we would like to note that, due to experimental drawbacks, EDXRD (the technique used in the studies where wolframite was found) is not the most accurate technique to solve an unknown crystal structure. Therefore, it is possible that the HP phase found under not hydrostatic conditions could have a structure similar to wolframite, but not exactly it. However, the crystal structure of that phase should not differ considerably from wolframite. What is clear after the present experiment is that in order to check rigorously whether a phase transition from scheelite to fergusonite or wolfamite occurs at HP the use of hydrostatic and non-hydrostatic HP conditions in comparable experiments is needed. However, the comparison of scheelite, fergusonite, and wolframite structures could shed light on the transition mechanisms.

In wolframite the coordination number of Ca decreases from eight in scheelite to six, but the coordination number of W increases from four to six. In contrast, the fergusonite structure (as scheelite) is built of WO_4 tetrahedra and CaO_8 dodecahedra. Indeed, fergusonite can be considered as a monoclinic distortion of scheelite **[17]**. In **Fig. 7** we show

the fergusonite structure of $CaWO_4$ to highlight its similitude to that of scheelite. In previous studies **[13, 14]** it was suggested that the scheeelite-to-fergusonite transition is caused by a slight distortion of WO_4 tetrahedra and a more important distorsion CaO_8 polyhedra, being at the phase transition the volume of WO_4 tetrahedra slightly enlarged and the volume of CaO_8 polyhedra reduced. These responses of both polyhedra were the consequences of a small decrease of two W-O bonds and the increase of the other two W-O bonds inside the WO_4 tetrahedra and the contraction of six of the Ca-O bonds in the CaO_8 polyhedra and the expansion of the remaining two. These facts are confirmed by the present experiment. On the other hand, in previous experiments no volume collapse at the scheeelite-to-fergusonite transition was observed **[13,14]**, and consequently it was proposed that this transformation could be a second-order phase transition **[17]**. However, in the present experiment a small volume discontinuity (~1%) is detected, pointing out to a first-order transition. Anyway, this discontinuity is smaller than the 2% volume collapse observed in the experiment in which the scheeelite-to-wolframite transition was found **[12]**. This is consistent with the suggestion that the scheelite to wolframite transformation increases the effective cation coordination with the consequent response to the demand of compression as a more efficient packing.

By comparing **Fig. 1** and **Fig. 7** it can be seen that fergusonite differs from scheelite basically by the fact that in fergusonite the cations form a zigzag chain where there is a small shift between the position of Ca and W. This fact can bring some light into the scheelite-fergusonite transition mechanism. Apparently, it can be attributed to small displacements of the Ca and W cations from their high-symmetry positions. This movement of the cations would induce changes in the O positions, polyhedra distortion, and a gradual tilting of the WO_4 tetrahedra. Nevertheless, in the fergusonite structure, certain features of the scheelite structure are conserved. Therefore, the scheelite-fergusonite transition can be considered as displacive, which is consistent with the small free energy difference between

both structures found by *ab initio* calculations **[14]**. After the transition, the monoclinic distortion of fergusonite $CaWO_4$ continuously increases from 10.4 GPa to 28 GPa as described above. As a consequence of it, the above described atomic displacements will be enhanced. A result of it is the augment of the splitting of Bragg peaks that can be seen by comparing the XRD patterns measured at 10.4 and 24.6 GPa (see **Fig. 2**). Another interesting consequence of the gradual changes induced by pressure in the fergusonite structure is the evolution of the tungsten coordination number from 4 at 10.4 GPa to 4 + 2 at 24.6 GPa. At this pressure, there are three double-degenerated W-O distances 1.742(9) Å, 1.743(9) Å, and 2.483(9) Å with the last distance only 7% larger than the average Ca-O bond distance, 2.312(9) Å, at the same pressure. It's likely, as in the case of $PbWO_4$ **[41]**, that the fergusonite structure may play the role of bridge phase between the scheelite structure, composed of WO_4 tetrahedra, and a HP structure containing WO_6 octahedra; like the orthorhombic structure predicted by theory **[14]** for pressures higher than those covered by experiments.

Figure 8 shows the wolframite structure of $CaWO_4$ which has been observed only under non-hydrostatic conditions **[12, 19]**. By comparing Fig. 8 with Fig. 1, it can be seen that in this case, the requested atomic displacements to transform scheelite into wolframite are quite important **[42]**. In particular, the transition involves the destruction of both the diamond-like structures of Ca and W cations of the scheelite structure and the formation of linear chains of either Ca or W atoms. Consequently the transition would be strongly reconstructive. This fact is consistent with the 7 GPa pressure range in which both scheelite and wolframite coexist **[19]**. It is also consistent with the fact that wolframite is only observed under non-hydrostatic conditions. In particular deviatoric stresses could induce the reconstruction of the structure required by the scheelite-wolframite transition **[42]**.

Concluding Remarks

We have studied $CaWO_4$ under compression at room temperature by means of XRD using synchrotron radiation. When compressed using Ne as PTM, we undoubtedly found that $CaWO_4$ transforms from its low-pressure tetragonal structure (scheelite) into a monoclinic structure (fergusonite). We have also determined the pressure evolution of the unit-cell parameters and unit-cell volume for the scheelite and fergusonite structures of $CaWO_4$. In scheelite compression is anisotropic, being the *c*-axis more compressible than the *a*-axis. A similar behavior is found in fergusonite, but in this case the unit-cell parameters show a strong non-lineal behavior. Additionally we found that the HP phase remains stable up to 28 GPa and that the phase transition is reversible with little hysteresis. A 1% volume change is detected at the transition supporting the occurrence of a first-order transformation. The experiments also provide information on the pressure evolution of interatomic bond distances and transition mechanisms. The results shed light on the influence of deviatoric stresses on the HP behavior of $CaWO_4$. These stresses affect the transition pressure and compressibility. In the extreme situation of highly non-hydrostatic conditions, they lead to HP phases other than fergusonite, as the wolframite structure **[12,19]**. This appears to be a common phenomenon in scheelite-structured oxides **[22,27]**.

Acknowledgments

Research sponsored by Spanish MINECO (MAT2010-21270-C04-01/04 and CSD2007-00045). Portions of this work were performed at HPCAT (Sector 16), Advanced Photon Source (APS), Argonne National Laboratory. HPCAT operations are supported by DOE-NNSA under Award No. DE-NA0001974 and DOE-BES under Award No. DE-FG02-99ER45775, with partial instrumentation funding by NSF. APS is supported by DOE-BES, under Contract No. DE-AC02-06CH11357.

References

[1] A.W. Sleight, Acta Crystallogr B **28**, 2899 (1972).

[2] A.A. Annenkov, M.V. Korzhik, and P. Lecoq, Nucl Instrum Methods Phys. Res. A **490** 30 (2002).

[3] M. Kobayashi, M. Ishi, Y. Usuki, and H. Yahagi, Nucl Instrum Methods Phys. Res. A **333**, 429 (1993).

[4] N. Faure, C. Borel, M. Couchaud, G. Basset, R. Templier, and R,C. Wyon, Appl. Phys. B **63**, 593 (1996).

[5] M. Nikl, P. Bohacek, N. Mihokova, M. Kobayashi, M. Ishii Y. Usuki, *et al*. J. Lumin. **87–89**, 1136 (2000).

[6] M. Nikl, P. Bohacek, N. Mihokova, N. Solovieva, A. Vedda, M. Martini, *et al*., J. Appl. Phys. **91**, 5041 (2002).

[7] A. Brenier,G. Jia, and Ch.Tu, J. Phys.: Condens. Matter **16**, 9103 (2004).

[8] R. M. Hazen, L. W. Finger, and J. W. E. Mariathasan, J. Phys. Chem. Solids **46**, 253 (1985).

[9] M. Nicol and J. F. Durana, J. Chem. Phys. **54**, 1436 (1971).

[10] A. Jayaraman, B. Batlogg, and L. G. van Uitert, Phys. Rev. B **28**, 4774 (1983).

[11] D. Christofilos, S. Ves, and G. A. Kourouklis, Phys. Stat. Sol. (b) **198**, 539 (1996).

[12] D. Errandonea, M. Somayazulu, and D. Haüsermann, Phys. Stat. Sol. (b) **235,** 162 (2003).

[13] A. Grzechnik, W.A. Crichton, M. Hanfland, and S. Van Smaalen, J. Phys.: Condens. Matter **15,** 7261 (2003).

[14] D. Errandonea, J. Pellicer-Porres, F.J. Manjon, A. Segura, Ch. Ferrer-Roca, R.S. Kumar, *et al*., Phys. Rev. B **72**, 174106 (2005).

[15] D. Errandonea, Phys. Stat. Sol. B **242**, R125 (2005).

[16] P. Rodríguez-Hernández, J.López-Solano, S. Radescu, A. Mujica , A. Muñoz , D. Errandonea, *et al*., J. Phys. Chem. Solids **67,** 2164 (2006).

[17] D. Errandonea, EPL **77**, 56001 (2007).

[18] Panchal, V; Garg, N; Chauhan, AK; et al., Sol. Stat. Comm. **130**, 203 (2004).

[19] Liu Ying-xin, Qin Shan, Li Xiao-dong, Li Yan-chun, and Liu Jing, Acta Mineralogica Sinica **29**, 524 (2009).

[20] R. Lacomba-Perales, D. Errandonea, A. Segura, *et al*., J. Appl. Phys. **110**, 043703 (2011).

[21] Li Yuqiang; Gao Yang; Han Yonghao; et al., J. Phys. Chem. C **116**, 25198 (2012)

[22] O. Gomis, J. A. Sans, R. Lacomba-Perales, D. Errandonea,Y. Meng, J. C. Chervin, and A. Polian Phys. Rev. B **86**, 054121 (2012).

[23] D. Errandonea and F. J. Manjon, Prog. Mater. Sci. **53**, 711 (2008).

[24] Y. Meng, D.J. Weidner, and Y. Fei, Geophysical Research Letters **20**, 1147 (1993).

[25] S. Klotz, J.C. Chervin, P. Munsch, and G. Le Marchand, J. Phys. D: Appl. Phys. **42**, 075413 (2009).

[26] D. Errandonea, Y. Meng, M. Somayazulu, and D. Häusermann, Physica B **355**, 116 (2005).

[27] D. Errandonea, L. Gracia, R. Lacomba-Perales, A. Polian, and J. C. Chervin, J. Appl. Phys. **113**, 123510 (2013).

[28] H. K. Mao, J. Xu, and P. M. Bell, J. Geophys. Res. **91**, 4673 (1986).

[29] A. P. Hammersley, S. O. Svensson, M. Hanfland, A. N. Fitch, and D. Häusermann, High Pressure Research **14**, 235 (1996).

[30] T. J. B. Holland, and S. A. T. Redfern, Mineralogical Magazine, **61**, 65 (1997).

[31] W. Kraus and G. Nolze, J. Appl. Crystallogr. **29**, 301 (1996).

[32] A. C. Larson and R.B. von Dreele, Los Alamos National Laboratory Report No. 86-748, 2004 (unpublished).

[33] D. Errandonea, O. Gomis, B. García-Domene, *et al.*, Inorg. Chem. **52**, 12790, (2013).

[34] A. Zalkin and D.H. Templeton J. Chem. Phys. **40**, 501 (1964).

[35] A.K. Singh, H.-P. Liermann,Y. Akahama, and H. Kawamura, J. Appl. Phys. **101**, 123526 (2007).

[36] A.B. Garg, D. Errandonea, P. Rodríguez-Hernández, S. López-Moreno, A. Muñoz, and C, Popescu, J. Phys.: Condens. Matter **26**, 265402 (2014).

[37] D. Errandonea, A. Muñoz, and J. Gonzalez-Platas, J. Appl. Phys. **115** , 216101 (2014).

[38] F. Birch, J. Geophys. Res. **83**, 1257 (1978).

[39] M.D. Frogley, J.L. Sly, D.J. Dunstan, Phys. Rev. B **58**, 12579 (1998).

[40] L Huiling, Z Shihong and Siyuan Z, J. of Solid State Chem. **180**, 589 (2007).

[41] D. Errandonea, J. Pellicer-Porres, F. J. Manjón, A. Segura, Ch. Ferrer-Roca, R. S. Kumar, O. Tschauner, J. López-Solano, P. Rodríguez-Hernández, S. Radescu, A. Mujica, A. Muñoz, and G. Aquilanti, Phys. Rev. B **73**, 224103 (2006).

[42] D. Errandonea, F. J. Manjón, M. Somayazulu, and D. Häusermann, J. Solid State Chem. **177**, 1087 (2004).

Table I: Structural parameters of scheelite-type and fergusonite-type $CaWO_4$ at different pressures. Atomic coordinates of scheelite are given with origin choice 2 for S.G. $I4_1/a$

Ambient pressure [34]: a = 5.243(2) Å, c = 11.376(3) Å

Atom	Site	x	y	z
Ca	4b	0	0.25	0.625
W	4a	0	0.25	0.125
O	16f	0.1504(13)	0.0085(14)	0.2111(6)

0.3 GPa: a = 5.236(4) Å, c = 11.356(6) Å, R_p = 2.6 %, R_{wp} = 2.9 %. Ne used as PTM

Atom	Site	x	y	z
Ca	4b	0	0.25	0.625
W	4a	0	0.25	0.125
O	16f	0.1794(9)	0.0065(9)	0.2022(9)

Structural parameters of $CaWO_4$ at 24.6 GPa. a = 5.150(4) Å, b = 10.442(8) Å, c = 4.839(4) Å, β = 95.07º R_p = 4.7 %, R_{wp} = 6.8 %. Ne used as PTM. Atomic coordinates of fergusonite are given with setting 13 for S.G. $I2/a$.

Atom	Site	x	y	z
Ca	4e	0.25	0.6003(9)	0
W	4e	0.25	0.1393(9)	0
O_1	8f	0.9212(9)	0.9644(9)	0.2321(9)
O_2	8f	0.4950(9)	0.2243(9)	0.8537(9)

Table II: EOS parameters at ambient pressure obtained for scheelite-type $CaWO_4$ from different studies. The pressure-transmitting media (PTM) and the pressure range of each experiment are indicated. ME (MEW) means methanol-ethanol (methanol-ethanol-water).

Pressure range (GPa)	**PTM**	**V_0 (Å^3)**	**B_0 (GPa)**	**B_0'**	**Ref.**
0 – 8.8	Ne	312.2(5)	83(3)	4.0[a]	This work
0 - 4.2	ME	312.6(4)	68(9)	4.0[a]	[8]
0 – 12	None	312.2(6)[b] 312.2[c]	77(8) 91(4)	4.9(9) 4.0[a]	[12]
0 - 9.5	He	312.5(6) 312.1(4)	68(6) 74(2)	5.59(1.65) 4.0[a]	[13]
0 - 10.8	Silicon oil	312.1(1) 312.2[c]	74(7) 78(2)	5.6(9) 4.0[a]	[14]
0 - 4.4	MEW	312.2[c]	78(7)	4.0[a]	[19]
0-10		314.3[d]	72[d]	4.3[d]	[16]

a B_0 fixed at 4.0.
b In **Ref. [12]** V_0 = 47 (0.26) in units of cm^3 mol$^{-1.}$
c V_0 fixed at 312.2 Å^3.
d *Ab initio* calculations.

Figure captions

Figure 1: (color online) Scheelite structure of $CaWO_4$. The bonds of the CaO_8 and WO_4 polyhedra are depicted.

Figure 2: (color online) Selected XRD patterns collected using Ne as pressure-transmitting medium. Rietveld refinements are shown for the scheelite structure at 0.3 GPa and for the HP fergusonite phase at 24.6 GPa with the experimental data plotted as solid lines and the calculated profiles as squares. In all of the cases the background has been subtracted. Residuals are also shown as solid lines. Vertical ticks indicate the position of Bragg reflections. Reflections of Ne are shown by arrows.

Figure 3: Selected XRD patterns of fergusonite $CaWO_4$. The numbers stand for pressures in GPa. The simulated positions of Bragg reflections of the XRD pattern at a pressure of 24.6 GPa are marked under it for fergusonite (F) and wolframite (W) structures. Miller indices are indicated for fergusonite at 24.6 GPa. The inset shows selected XRD patterns of the scheelite phase at different pressures where the (101), (112) and (103) reflections are marked.

Figure 4: (color online) Pressure evolution of the lattice parameters, unit-cell volume, and c/a axial ratio obtained from different experiments using different PTM. Red circles refer to our experiments carried out with Ne as PTM, green rhombs refer to data without PTM from **Ref. [12]**, dark yellow stars refer to data with methanol-ethanol as PTM from **Ref. [8]**, blue squares refer to data with He as PTM from **Ref. [13]**, magenta up triangles refer to data with silicon oil as PTM from **Ref. [14]** and cyan right triangles refer to 16:3:1 methanol-ethanol-water as PTM **Ref. [19]**. Solid lines are quadratic fits included only for the sake of following the tendencies

Figure 5: (color online) Pressure dependence of the interatomic bond distances in the scheelite phase of $CaWO_4$. Red solid circles represent the distances in the scheelite phase here reported, magenta solid triangles (**Ref. [14]),** green solid rhombs (**Ref. [12]),** dark yellow solid stars and asterisks (measurements outside the DAC) (**Ref. [8])** represent the distances in the scheelite phase reported in the literature. Solid lines are linear fits included in order to show the tendencies.

Figure 6: (Color online) Pressure evolution of the experimental lattice parameters (and volume) of the (tetragonal) scheelite and (monoclinic) fergusonite phases of $CaWO_4$: solid and void red circles (our measurements) with Ne as PTM, solid and void blue up squares with He as PTM (**Ref. [13]**), solid and void magenta up triangles with silicon oil as PTM (**Ref. [14]**), solid green rhombs without PTM (**Ref. [12]**), solid dark yellow stars with methanol-ethanol as PTM (**Ref. [8]**) and solid cyan right triangle with 16:3:1 methanol-ethanol-water as PTM (**Ref. [19]**). For the volume-pressure data, the red lines represent the EOS of the scheelite and fergusonite phases. The evolution of the β angle versus pressure for the fergusonite phase is reported in an inset.

Figure 7: (color online) Fergusonite structure of $CaWO_4$. The bonds of the CaO_8 and WO_4 polyhedra are depicted.

Figure 8: (color online) Wolframite structure of $CaWO_4$. The bonds of the CaO_6 and WO_6 polyhedra are depicted.

Figure 1

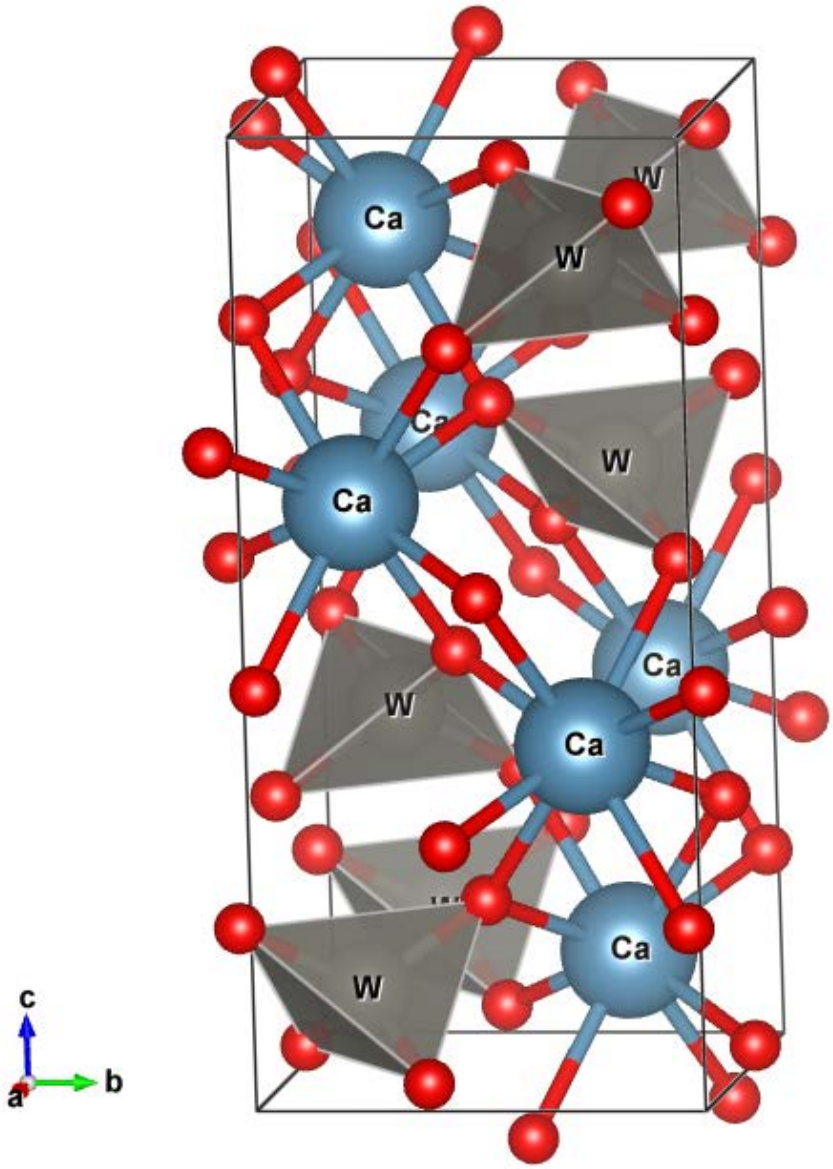

Figure 2

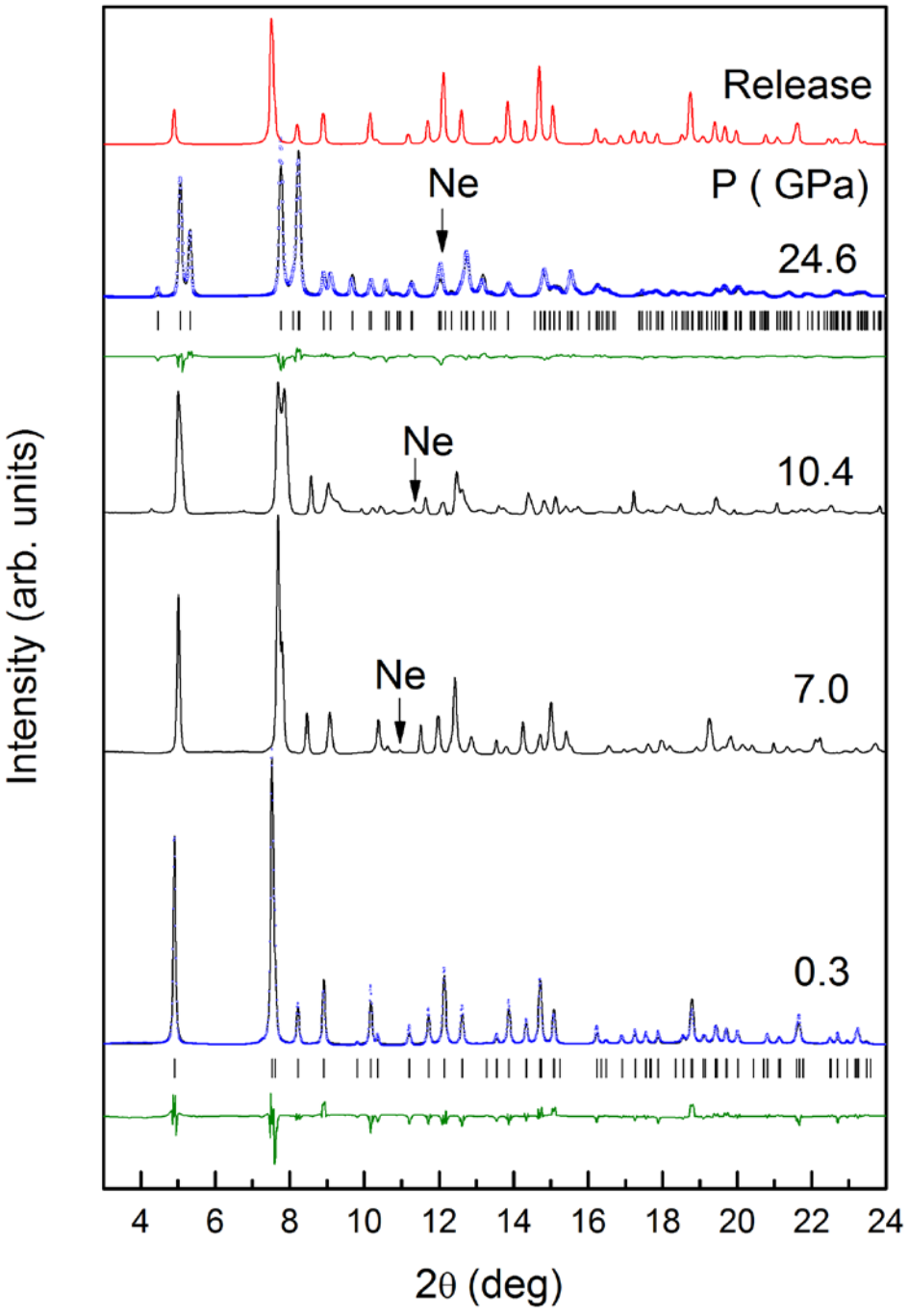
Release
Ne
P (GPa)
24.6
Ne
10.4
Ne
7.0
0.3
Intensity (arb. units)
4
6
8
10
12
14
16
18
20
22
24
2θ (deg)

Figure 3

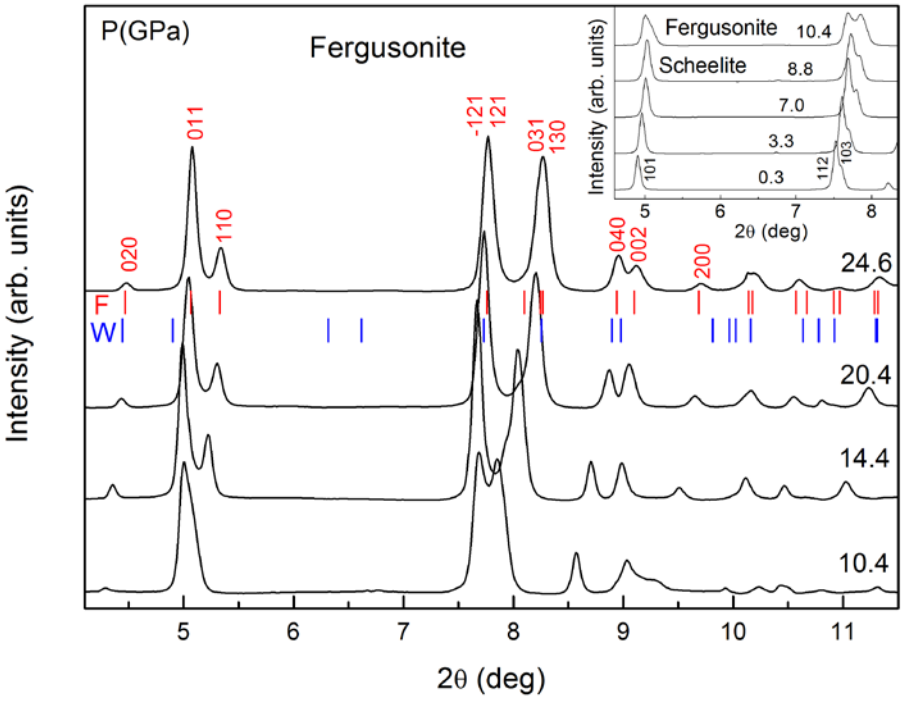
P(GPa)
Fergusonite
Intensity (arb. units)
020
011
110
-121
121
031
130
040
002
200
24.6
20.4
14.4
10.4
F
W
2θ (deg)
Fergusonite 10.4
Scheelite 8.8
7.0
3.3
0.3
101
112
103

Figure 4

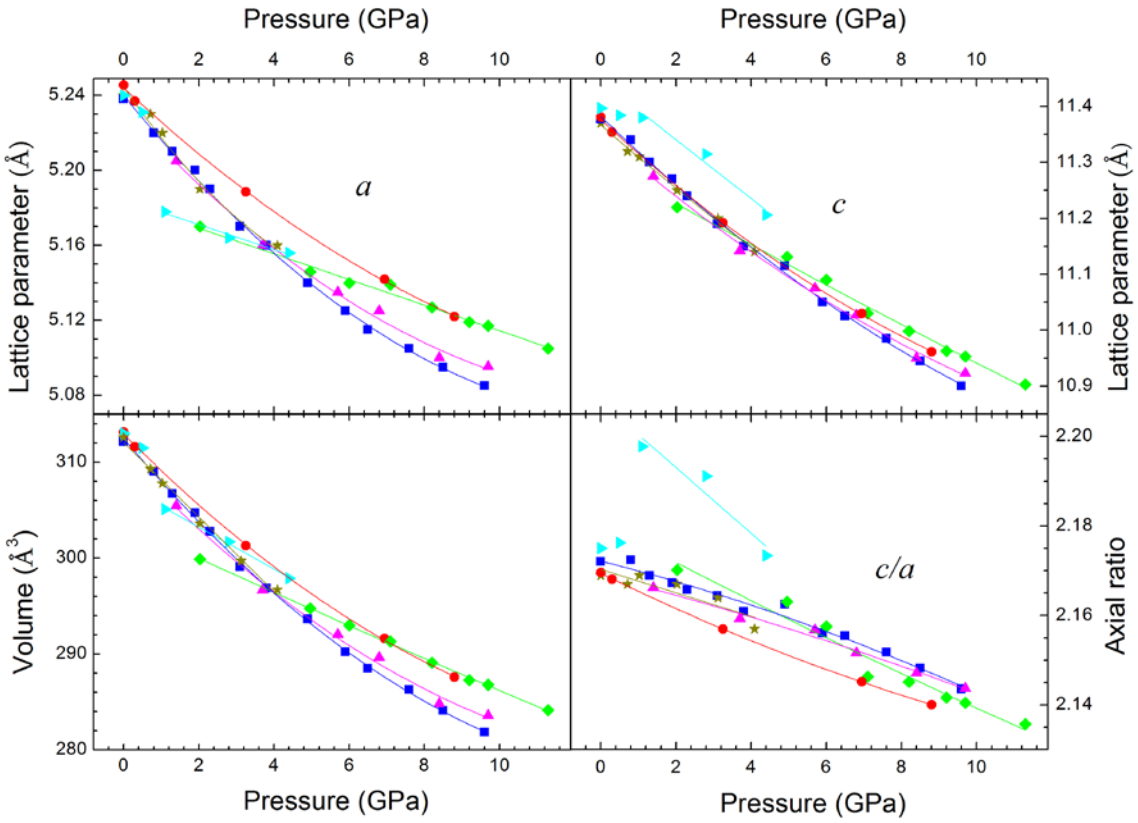
Pressure (GPa)
Pressure (GPa)
Lattice parameter (Å)
a
c
Lattice parameter (Å)
Volume (Å3)
c/a
Axial ratio
Pressure (GPa)
Pressure (GPa)

Figure 5

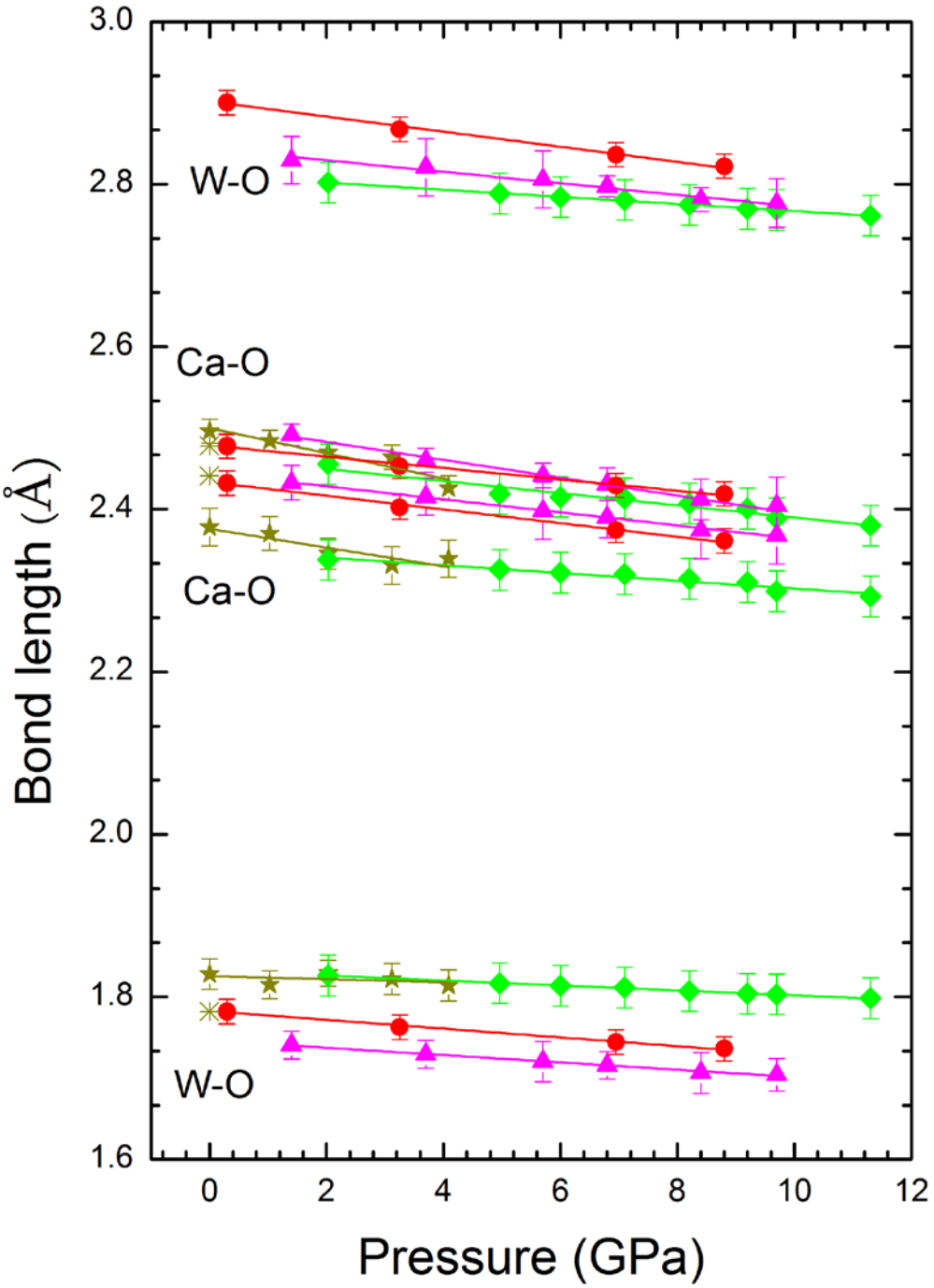
3.0
2.8
2.6
2.4
2.2
2.0
1.8
1.6
Bond length (Å)
W-O
Ca-O
Ca-O
W-O
0
2
4
6
8
10
12
Pressure (GPa)

Figure 6

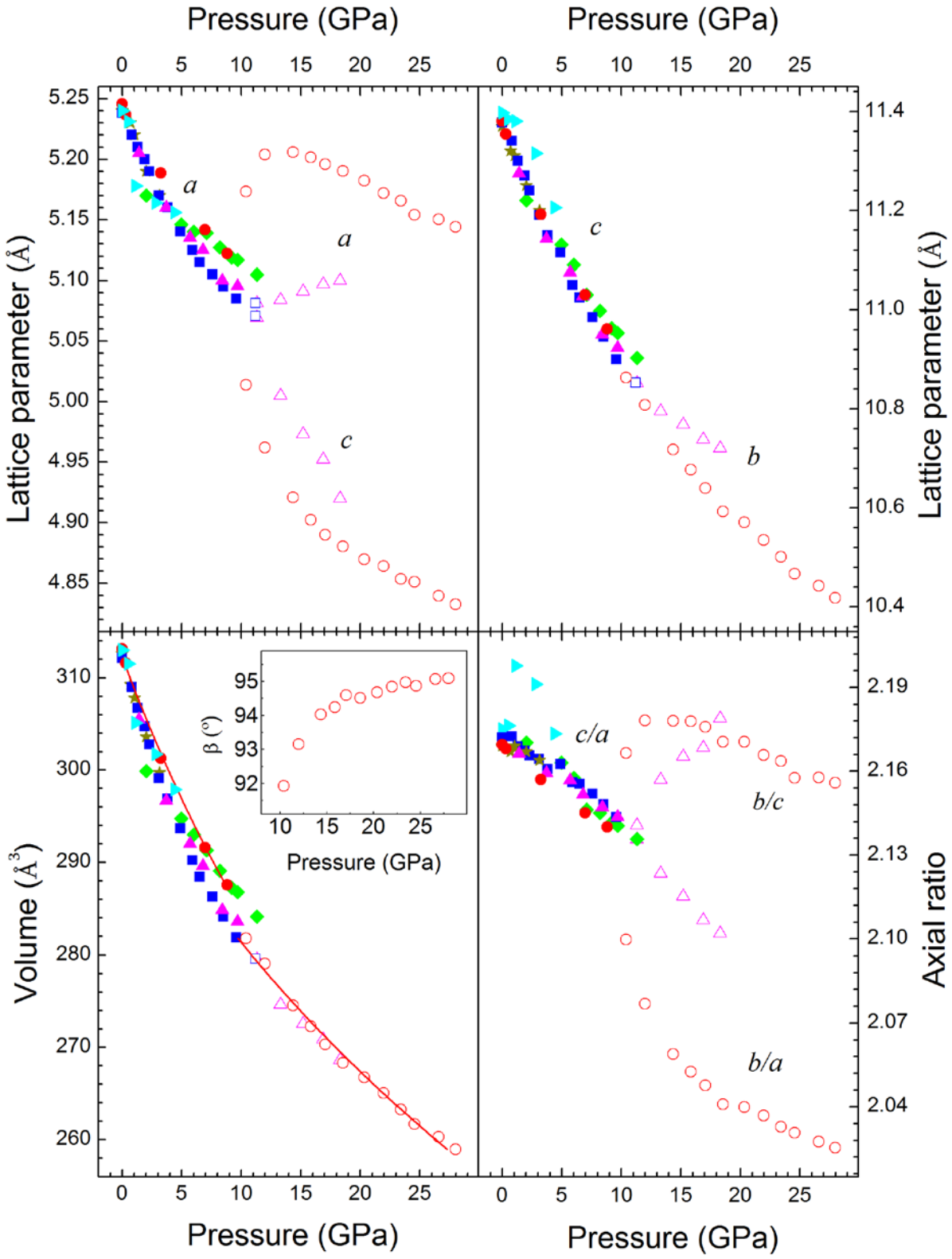
Pressure (GPa)
Pressure (GPa)
Lattice parameter (Å)
a
a
c
c
b
Lattice parameter (Å)
Volume (Å3)
β (°)
Pressure (GPa)
c/a
b/c
b/a
Axial ratio
Pressure (GPa)
Pressure (GPa)

Figure 7

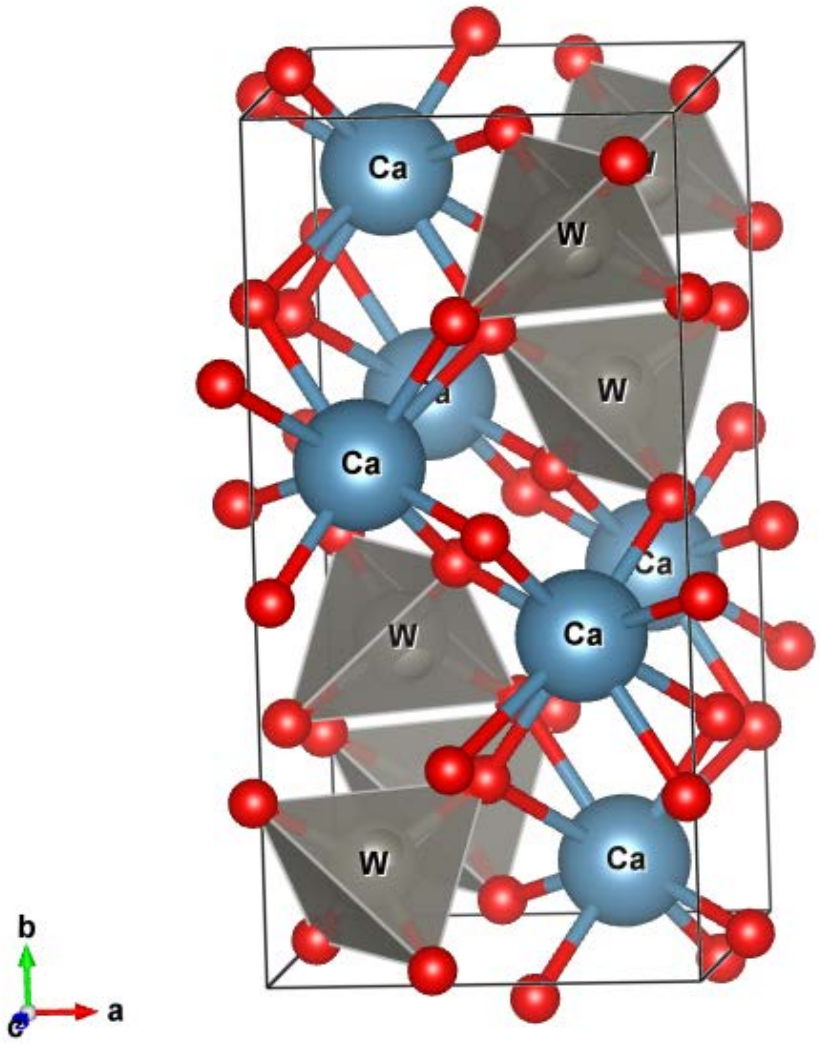

Figure 8